

Anisotropic dissociation of NO in *K*-shell excited states

Norio Saito and Isao H. Suzuki

Electrotechnical Laboratory, 1-1-4, Umezono, Tsukuba-shi, Ibaraki, 305 Japan

(Received 18 December 1989; revised manuscript received 28 March 1990)

The angular distributions of fragment ions produced from NO in N *K*-shell or O *K*-shell excited states have been measured with a rotatable time-of-flight mass spectrometer. The asymmetry parameter (β) derived from the measured angular distribution is -0.75 at 399.7 eV (N $1s \rightarrow \pi^*$). The β parameter for transitions of the N $1s$ electron to Rydberg orbitals changes with the symmetry of the transitions. The β parameter shows a broad maximum around 415 eV due to a σ^* shape resonance. The β parameter for O $1s$ excitation is similar to that for N $1s$ excitation.

I. INTRODUCTION

There have been a number of studies on the measurement and interpretation of inner-shell excitation spectra of molecules.¹⁻³ Inner-shell spectra of unsaturated diatomic molecules are characterized by two kinds of resonances (π^* and σ^*) and by transitions to Rydberg orbitals. The lower-energy π^* resonance occurs appreciably below the inner-shell ionization potential (IP). The higher-energy σ^* resonances may be positioned below or above the IP. For clear determination of symmetry for these transitions, it is useful to measure angular distributions of fragment ions produced from molecules in inner-shell excited states.⁴ Very recently, anisotropy in the ionic fragmentation from *K*-shell excited molecules, N₂ (Refs. 5-7) and O₂ (Ref. 8), has been measured with angle-dependent photoionization spectrometry. This new technique determines molecular orientation at the instant of photoabsorption when the lifetime of the dissociation is fast relative to any disorienting process.

After the inner-shell excitation of a molecule, an Auger-type transition occurs, producing a highly-valence-excited molecular ion which, in turn, decomposes into fragment ions.⁹ The Auger transition and subsequent ionic fragmentation generally occur much faster than the rotational motion of the molecule since the highly-valence-excited states have repulsive potential curves in most cases.¹⁰ Therefore fragment ion angular distributions can be a powerful tool for determining transition symmetry through the molecular orientation at the initial photoabsorption step.

Photoabsorption spectra^{11,12} and an electron-energy-loss spectrum¹³ of NO show fine structures near the N *K* and the O *K* edges. In the region of the N *K* edge, an intense peak attributed to the N $1s \rightarrow 2p \pi^*$ transition appears at 399.7 eV. [The states $(1s)^{-1}{}^3\Pi(2p \pi^*)^1$ and $(1s)^{-1}{}^1\Pi(2p \pi^*)^1$ have not been resolved experimentally.] Ionization thresholds are located at 410.3 eV for ${}^3\Pi$ and at 411.8 eV for ${}^1\Pi$. There are weak peaks between the intense peak and the ionization thresholds, which correspond to excitations of N $1s$ electrons to discrete Rydberg orbitals. Above the ionization thresholds, a broad band is located around 415 eV, which is interpreted

ed to originate from a σ^* shape resonance. The absorption spectrum near the O *K* edge is similar to that near the N *K* edge.

In order to examine the interpretation of NO core-level photoabsorption spectra in detail, angular distributions of fragment ions (N⁺, O⁺, N²⁺, and O²⁺) produced from NO following soft-x-ray absorption have been measured in the region of the N *K* and the O *K* edges using a rotatable time-of-flight (TOF) mass spectrometer.

II. EXPERIMENT

The experimental procedure has been described elsewhere.^{5,7} Briefly, synchrotron radiation from an electron storage ring at the Electrotechnical Laboratory¹⁴ was dispersed with a Grasshopper monochromator.¹⁵ The resolving power of the monochromator ($\lambda/\Delta\lambda$) was estimated to be about 500 in the N *K*-edge region and about 300 in the O *K*-edge region. The monochromatized soft x-rays crossed an effusive NO beam at right angles in the center of the TOF mass spectrometer. The purity of NO molecules was 99.9%. The electrons and ions produced by soft-x-ray irradiation were extracted in opposite directions and detected with microchannel plates.¹⁶ The detected signals were processed with a combination of usual nuclear-instrument modules. TOF spectra of fragment ions have been measured using the mass spectrometer in a photoelectron-photoion coincidence mode at angles of 0° , 54.7° , and 90° with respect to the polarization direction of the incident photon. (All electrons having various energies can make a start signal for TOF spectra.) An electric field (13 or 26 V/mm) was applied to the interaction region in the spectrometer.

III. RESULTS AND DISCUSSION

A. Experimental results

Figure 1 shows TOF spectra of the combined N⁺, NO²⁺, and O⁺ signal measured at photon energies of 399.7 , 406.4 , and 414.6 eV at angles of 0° and 90° . These energies correspond to the excitations of a N $1s$ electron to $2p \pi^*$, $3s \sigma$, and the shape resonance, respectively. On the basis of a fitting calculation described below, struc-

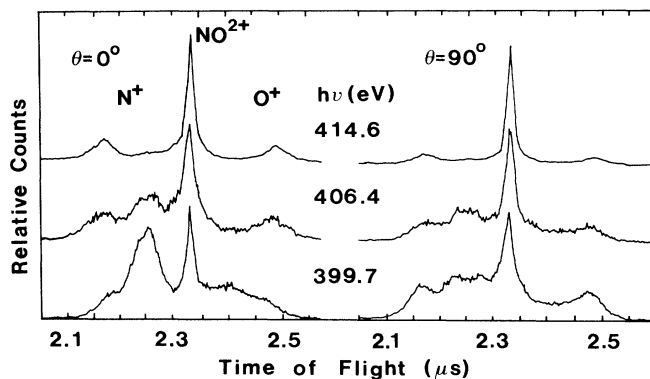


FIG. 1. TOF spectra of N^+ , NO^{2+} , and O^+ from NO measured at photon energies of 399.7, 406.4, and 414.6 eV for spectrometer angles of 0° (left) and 90° (right).

tures in the TOF spectra are interpreted as follows. A broad peak around $2.16 \mu s$ is produced by N^+ ions initially moving toward the ion detector with a kinetic energy of about 5 eV. A peak around $2.25 \mu s$ originates from N^+ having a low kinetic energy (~ 1 eV). Although there is usually a possibility that N^+ ions with 5 eV initially moving in a direction perpendicular to the spectrometer axis contribute to the peak at $2.25 \mu s$, the ions cannot reach the detector under the present experimental conditions (small aperture size and weak electric field). A central peak at $2.33 \mu s$ originates from three contributions: NO^{2+} ions with thermal kinetic energy, which produce a sharp peak, N^+ ions with about 5 eV kinetic energy initially moving away from the ion detector and repelled back toward the detector by the extraction field, and O^+ ions with about 4 eV kinetic energy initially moving toward the ion detector. A peak around $2.47 \mu s$ is produced by O^+ ions initially moving away from the ion detector with about 4 eV kinetic energy.

At the $1s \rightarrow 2p \pi^*$ excitation (399.7 eV), the TOF spectrum measured at 0° shows a peak at $2.25 \mu s$ generated by N^+ ions with a low kinetic energy and shoulders at 2.16 and $2.47 \mu s$, respectively, originating from the N^+ and the O^+ ions with high kinetic energies. In contrast the spectrum measured at 90° has a much different profile, indicating that the intensities of the shoulders at 2.16 and $2.47 \mu s$ increase and the intensity of the peak at $2.25 \mu s$ decreases. This qualitative finding suggests that the molecule preferentially dissociates in the direction perpendicular to the photon polarization: The excitation at 399.7 eV is a $\Pi \rightarrow \Sigma$ or $\Pi \rightarrow \Delta$ transition ($1s \sigma \rightarrow 2p \pi^*$ transition in the one-particle picture).

B. Analysis of TOF spectra

In order to determine angular distribution parameters (β) from the angle-dependent TOF spectra, simulation calculations have been carried out. This procedure is briefly presented here because a detailed description was reported elsewhere.^{7,16} In a simple case where a monoenergetic fragment ion emerges from a point source, the TOF spectrum is expressed as

$$f(t, \theta, \beta) \propto 4 + \beta(1 - 3 \cos^2 \theta) \{1 - 3[(t - t_0)/\Delta t]^2\} \quad (1)$$

for $t_0 - \Delta t < t < t_0 + \Delta t$, where t , t_0 , and Δt denote the flight time of the ion with kinetic energy, the flight time of the ion with no kinetic energy, and a half of the full width at the base of the TOF spectrum derived from the kinetic energy, respectively. In this equation, θ denotes the angle between the TOF spectrometer axis and the polarization vector of the incident photon. The half width Δt is connected with the applied electric field (E) as follows:

$$\Delta t = \frac{\sqrt{2mW}}{qE}, \quad (2)$$

where m denotes the mass of the fragment ion, W indicates the kinetic energy of the ion, and q is the electric charge of the ion.

The observed TOF spectrum is determined by the kinetic-energy distribution and the angular distribution of the dissociating ion, the characteristics and the geometrical orientation of the TOF mass spectrometer, and the applied electric fields. The latter two factors are set at a fixed value in the measurements. The undetermined factor necessary for derivation of the angular distribution is the kinetic-energy distribution of the fragment ion. Fortunately, the TOF spectrum of the fragment ion taken at 54.7° (magic angle) is almost the same as that of isotropic dissociation ($\beta=0$), even if the ion source is not a point (i.e., a line along the photon beam in the present measurement) and if the polarization degree of the photon slightly deviates from 100%. In fact, the calculated TOF spectrum changes at most by 1% at the magic angle as β changes from -1 to 2 . Therefore the kinetic-energy distribution has been determined from the TOF spectrum at 54.7° by the simulation calculation, assuming that $\beta=0$. In this simulation, the trajectory of the fragment ion was calculated inside the TOF spectrometer and the effect of the angular resolution on each kinetic energy was taken into account. Values of kinetic energies were selected such that the term \sqrt{W} changed at a constant step, yielding widths of TOF spectra that change at a constant step in the time scale (i.e., about $0.25 \mu s$). The simulation calculation gave the weight factor to each kinetic energy, which corresponds to the distribution of kinetic energies after correction of collection efficiency of ions. Another choice of group of kinetic energies yielded essentially the same profile of kinetic-energy distribution. Effective angular resolution and detector efficiency for different kinetic energies have been considered in the present simulation technique.

Figure 2 shows the TOF spectra calculated for N^+ , O^+ , and NO^{2+} ions at 399.7 eV taken at 54.7° , 0° , and 90° . The β parameter was assumed to be 0 for the spectrum at 54.7° and -0.7 for those at 0° and 90° . The dashed curves at the bottom (centered at $2.42 \mu s$) are calculated profiles of O^+ ions with several kinetic energies. The dashed curves second from the bottom (centered at $2.25 \mu s$) are calculated profiles of N^+ ions with several kinetic energies. The dashed curve with the 54.7° spectrum (centered at $2.33 \mu s$) is a calculated profile of NO^{2+} ions with thermal energy. The solid curve for 54.7° is the sum

of all of these dashed curves. Profiles of N^+ ions with about 5 eV, of NO^{2+} ions with thermal energy, and of O^+ ions with about 4 eV overlap one another at $2.33 \mu s$. Only solid curves are drawn for the spectra at 0° and 90° . Each dashed curve in the figure represents the relative collection efficiency for all ions with a particular kinetic energy as a function of initial emission angle. The ions initially moving toward the ion detector correspond to a shorter value of the flight time in the dashed curve. On the other hand, the ions initially moving away from the detector yield a longer flight time. The ions initially moving perpendicular to the spectrometer axis contribute to the center of the dashed curve. When the kinetic energy becomes high, the intensity at the center of the dashed curve becomes low. This fact shows that the collection efficiency of the ions initially moving perpendicular to the axis is lower for higher kinetic energy.

This figure shows that the calculated profile at 54.7° has well reproduced the experimental data. The kinetic-

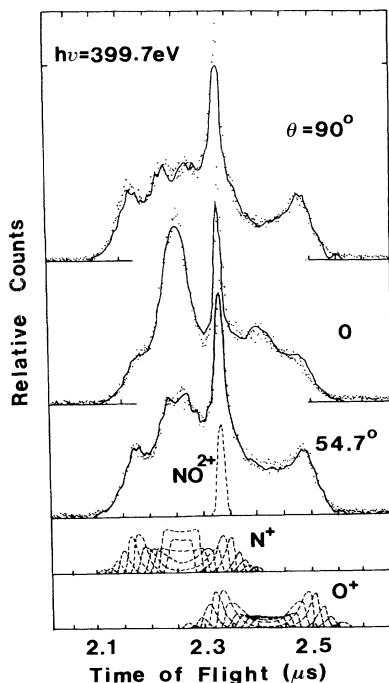


FIG. 2. Experimental and calculated spectra of N^+ , NO^{2+} , and O^+ at 54.7° , 0° , and 90° measured at 399.7 eV. Dots are the experimental data. Dashed curves at the bottom (centered at $2.42 \mu s$) are the profiles of O^+ ions derived from the simulation calculation on the assumption that $\beta=0$ and the kinetic energies are 0.315, 0.709, 1.26, 1.97, 2.81, 3.86, 5.04, 6.36, 7.88, 9.48, and 11.34 from inner to outer. Dashed curves at the second column from the bottom (centered at $2.25 \mu s$) are the calculated profiles of N^+ ions on the assumption that $\beta=0$ and the kinetic energies are 0.36, 0.81, 1.44, 2.25, 3.21, 4.41, 5.76, 7.27, 9.0, 10.83, and 12.96 eV from inner to outer. A dashed curve at the third column from the bottom (centered at $2.33 \mu s$) is the calculated profile of NO^+ ions on the assumption that $\beta=0$ and the kinetic energy is thermal. The solid curve for 54.7° is the sum of these dashed curves. The solid curves for 0° and 90° are profiles calculated on the assumption of $\beta=-0.7$.

energy distribution of N^+ obtained shows a maximum at about 5 eV at every photon energy. That of O^+ shows a maximum at about 4 eV. These results seem reasonable in the light of molecular ion states populated through Auger processes.¹⁷ The kinetic-energy distribution at the energy of the $N K \rightarrow \pi^*$ transition shows considerable intensity at about 0.5 eV. In K -shell excitation of N_2 (and also O_2), atomic ions having kinetic energies of 0.5–1.0 eV are produced at the $K \rightarrow \pi^*$ transition. These ions were ascribed to come from dissociation processes like $N_2(K^{-1}\pi^*) \rightarrow N_2^+(V^{-1} \text{ and } V^{-2}\pi^*) + e \rightarrow N^+ + N + e$, where V refers to a valence orbital.^{16,18,19} In the present case of NO , a similar phenomenon is presumed to occur. These results will be discussed in another publication.

After the kinetic-energy distribution was obtained, the TOF spectra at 0° and 90° were reproduced by calculation with various β values. In this calculation, the photon was assumed to be 100% linearly polarized. The β value was determined to minimize the difference between the experimental data and the calculated profile. Examples of the simulation are shown in Fig. 2.

The β parameters obtained from the data at 0° and 90° are in agreement with each other. The data at different applied electric fields (13 and 26 V/mm) gave the same value to the parameter within the uncertainties considered. If the applied electric field has an effect on molecular orientation, the field would cause different values for the β parameter to be derived from TOF spectra at different angles and/or at different fields. Therefore the field has no measurable effect on the derived β values. Since signals for N^+ , O^+ , and NO^{2+} ions were not separated in the TOF spectra as shown in Fig. 1, it was difficult to obtain each β parameter for N^+ and O^+ ions accurately. Thus the authors have calculated a mixing of the β parameter for N^+ and O^+ ions [$\beta_e(1)$] and that for N^{2+} and O^{2+} [$\beta_e(2)$].

C. Asymmetry parameter

Figure 3 shows the asymmetry parameters mixed for N^+ and O^+ (in the middle), and for N^{2+} and O^{2+} (at the bottom) in the $N K$ -edge region, together with the electron yield spectrum (at the top). This electron yield spectrum shows a similar profile to the photoabsorption spectrum by Akimov, Vinogradov, and Zimkina¹¹ and has a slightly different character from the data by Morioka *et al.*¹² and Wight and Brion.¹³ There is no observable structure near the energy of 404 eV in the present spectrum. This result supports the argument by Akimov, Vinogradov, and Zimkina that the structures appearing near 404 eV in the spectra by the latter two groups can be ascribed to impurity effects. The β parameter for N^+ and O^+ and that for N^{2+} and O^{2+} show essentially the same photon energy dependence. This result suggests that intermediate states for production of the singly and doubly charged ions have the same lifetime or a shorter lifetime than the rotational motion within the accuracy considered.

The β parameter shows an oscillatory variation below the $N K$ edge and increases to a broad maximum around 414 eV above the $N K$ edge. It is interesting to compare

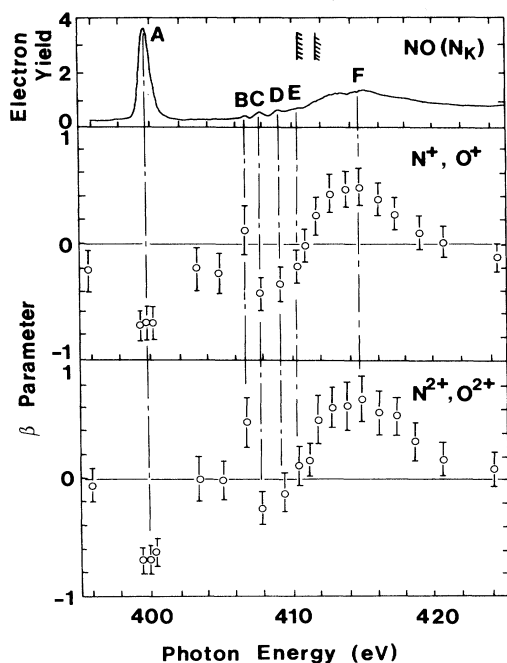


FIG. 3. Asymmetry parameters for N^+ and O^+ and for N^{2+} and O^{2+} as a function of photon energy near the N K edge, together with the yield of the total electron signals. Bars indicate sizes of experimental uncertainties. Symbols A–F were put for clarity of discussion in the text. The bars with hatching denote the ionization threshold for $^3\Pi$ (left-hand side) and that for $^1\Pi$.

the measured asymmetry parameters with the predicted electronic transitions. The β parameters obtained by the experiment include effects due to photoionization of valence electrons by the soft x-rays and by stray light. Thus the measured β parameter has been corrected by subtracting the effect of underlying valence ionization. Table I lists the β parameter results below the N K edge. The parameter for singly charged ions $\beta_e(1)$ is slightly different from that for doubly charged ions [$\beta_e(2)$] at peaks C–E. However, this difference is smaller than the sizes of error considered.

The value of $\beta_e(1)$ is utilized for discussion below be-

cause the signal intensity of the singly charged ions is higher than that of the doubly charged ones. The β parameter at peak A ($1s \rightarrow 2p \pi^*$) is about -0.75 ± 0.2 . (The value, -0.75 , is the average value obtained with several measurements.) This value is close to the expected value of -1 for $\Pi \rightarrow \Sigma$ and $\Pi \rightarrow \Delta$ transitions in consideration of the present uncertainty. The slight discrepancy may come from the following factors. First, polarization of the incident soft-x-ray beam was not 100% owing to the present optical system. The degree of polarization was estimated to be 93% by calculation. In this estimation, the β value of -1 corresponds to a measured value of -0.95 , which agrees with the present value within the uncertainty. The other possible factor is an effect of the rotational motion of the excited ionic molecule. The doubly charged ion of NO has stable potentials as well as the singly ionized ion.²⁰ These potentials can reduce the average speed of dissociation over various channels, because part of the fragment ions are produced through predissociation from a stable potential.

The β value at peak B ($1s \rightarrow 3s \sigma$) is 1.0 ± 0.5 . The value expected for a $\Pi \rightarrow \Pi$ transition is 2. The discrepancy between the obtained and the expected β values is probably connected with the factors mentioned above. The imperfect polarization of the photon (93%) gave a β value of 1.9 instead of 2. A surface contamination of optical elements used has occasionally an effect on a polarization degree of the photon and decreases it. Rotational effects, however, seem to be more important for the discrepancy in the β parameter at peak B. With these considerations, the present value is consistent with the assignment of peak B to the $1s \rightarrow 3s \sigma$ transition. At peaks C ($1s \rightarrow 3p \pi$ and $3s \sigma'$) and D ($1s \rightarrow 4s \sigma$, $3p \pi'$, and $3d$), the β parameters are -0.6 and -0.5 , respectively. It is presumed that the cross section of $1s \rightarrow 3p \pi$ is higher than that of $1s \rightarrow 3s \sigma$ or $4s \sigma$, on analogy with the case of N_2 .¹ The negative β values at peaks C and D are reasonable. At peak E ($1s \rightarrow 4s \sigma'$ and $3d'$), the β parameter is -0.2 . Since transitions to higher Rydberg orbitals and into the $(1s)^{-1}$ continuum might occur at this photon energy owing to the low photon-energy resolution, the β parameter is consistent with the expected value.

Above the ionization threshold, the β parameter rises to 0.65 at 414 eV and gradually decreases with an increase in photon energy. The electron yield spectrum

TABLE I. Asymmetry parameter for photoexcitation of the N 1s electron of NO. β_e is the experimental value corrected by subtracting the effect of valence photoionization. The digit in parentheses (1 or 2) means that the β_e is for singly charged ions or doubly charged ones.

Peak	Energy (eV)	Excited orbital ^a		$\beta_e(1)$	$\beta_e(2)$
		$^3\Pi$ ^b	$^1\Pi$ ^c		
A	399.7	$2p \pi^*$	$2p \pi^{*}$	-0.75 ± 0.2	-0.75 ± 0.2
B	406.4	$3s \sigma$		1.0 ± 0.5	0.9 ± 0.5
C	407.6	$3p \pi$	$3s \sigma'$	-0.6 ± 0.3	-0.3 ± 0.3
D	408.9	$4s \sigma, 3d$	$3p \pi'$	-0.5 ± 0.3	-0.2 ± 0.3
E	410.2		$4s \sigma', 3d'$	-0.2 ± 0.3	0.1 ± 0.3

^aReference 11.

^bTriplet ionization state [$N(1s)^{-1}$] at 410.3 eV.

^cSinglet ionization state [$N(1s)^{-1}$] at 411.8 eV.

shows a similar behavior. In comparison of inner-shell excitation spectra of related molecules,^{3,11} this broad maximum in the excitation spectra was interpreted to come from a σ -type shape resonance effect. If this shape resonance occurs there, the β parameter is supposed to show a positive value owing to the $1s \sigma \rightarrow \sigma^*$ transition. The present result on the broad maximum of the β parameter confirms the previous interpretation that the σ^* shape resonance state peaks around 414 eV.

The asymmetry parameters mixed for N^+ and O^+ and for N^{2+} and O^{2+} in the O K -edge region are shown as a function of photon energy in Fig. 4, together with the total electron yield spectrum. The obtained electron yield spectrum does not clearly exhibit peaks associated with transitions from $1s$ to Rydberg orbitals. The background intensity of the electron yield spectrum in Fig. 4 is higher than that in Fig. 3. This is because ionization of the N $1s$ shell contributes appreciably to this background and the photon beam includes more stray light than in the N K region.

However, the electron yield spectrum shows a peak at 532.5 eV and a broad maximum above the O K edge. The feature is similar to the spectrum by Akimov, Vinogradov, and Zimkina.¹¹ The β parameter at a photon energy of 532.5 eV ($O 1s \rightarrow 2p \pi^*$) is -0.6 , which corresponds to a corrected value of -0.9 by subtracting

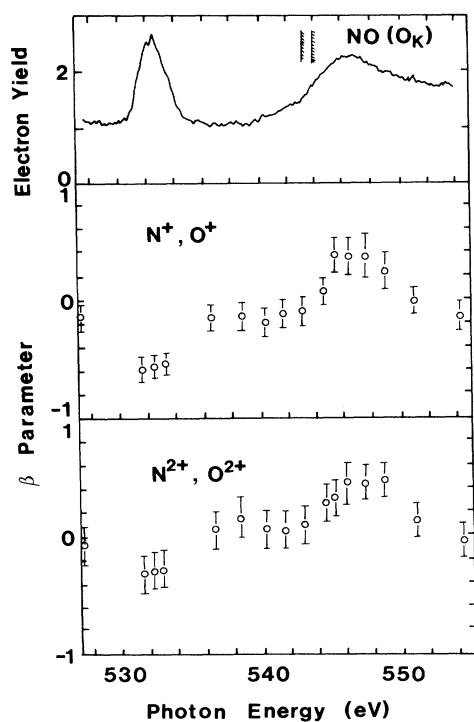


FIG. 4. Asymmetry parameters for N^+ and O^+ and for N^{2+} and O^{2+} as a function of photon energy near the O K edge, together with the yield of the total electron signals. Bars indicate sizes of experimental uncertainties. The bars with hatching denote the ionization threshold for $^3\Pi$ (left-hand side) and that for $^1\Pi$.

effects of valence ionization and of N $1s$ ionization. This value is in agreement with the expected value of -1 for $\Pi \rightarrow \Sigma$ and $\Pi \rightarrow \Delta$ transitions. At photon energies from 538 to 543 eV (transitions from O $1s$ to Rydberg orbitals), the β parameter is close to zero. This result comes from the following explanation. Ionizations of the N $1s$ electron and of the valence electron are dominant in comparison with the excitation of the O $1s$ electron. The photon-energy resolution is low, making transitions to Rydberg states overlap one another.

Above the ionization threshold ($^3\Pi$: 543.3 eV), the β parameter rises to about 0.4 (a corrected value of 0.75 for only O $1s$ excitation) at 546 eV and gradually decreases with increasing photon energy. The energy position of the maximum β value is in agreement with that of the electron yield spectrum. This broad maximum near 546 eV is associated with the σ^* shape resonance. The position of the maximum β value related to the O K edge is slightly lower than that at the N K edge. The width of the shape resonance at the O K edge is narrower than that at the N K edge.

It is important to compare the obtained β parameter of NO with those of related molecules (N_2 and O_2) for comprehensive understanding of the character of K -shell excited states. Table II lists the excited orbitals and the corresponding β parameters of N_2 ,^{5,7} O_2 ,⁸ and NO. For π^* excitation, the β parameters are in agreement with one another within uncertainties for the three molecules. For $3s$ excitation, the parameter of N_2 is 1.4 ± 0.3 , being close to the expected value, 2 ($1s \sigma \rightarrow 3s \sigma$). That of NO is 1.0 ± 0.5 , being slightly different from the expected value. This difference may be connected with the open-shell structure of NO. The β parameter of O_2 is 1.4 ± 0.3 , close to expectation ($1s \sigma \rightarrow 3s \sigma$ and σ^* shape resonance).

The parameter of O_2 for $3p$ excitation is 1.23 ± 0.2 , which is much different from those of N_2 and NO (about -0.65). In the latter two molecules, the dominant transition is presumed to be $1s \sigma \rightarrow 3p \pi$. In contrast, the σ^* shape resonance occurs at this energy for O_2 , yielding a positive β value. At the $3d$ (and $4s$) excitation, a similar difference is seen among the β parameters of these molecules. The β parameter of O_2 is positive (1.05), and those of N_2 and NO are negative (about -0.5). This is also because the shape resonance is in this energy region in O_2 .

The comparison of the β parameter and of the antibonding orbital energy among the three molecules has

TABLE II. Asymmetry parameter for transitions to discrete orbitals below the K edge in N_2 , O_2 , and NO. An orbital in parentheses means that a transition to this orbital overlaps with that to the orbital listed at left.

Orbital	β parameter		
	N_2	O_2	NO(N K)
π^*	-0.71 ± 0.15	-0.89 ± 0.15	-0.75 ± 0.2
$3s$	1.4 ± 0.3	1.41 ± 0.2 (σ^*)	1.0 ± 0.5
$3p$	-0.66 ± 0.2	1.23 ± 0.2 (σ^*)	-0.6 ± 0.3 ($3s'$)
$3d$ and $4s$	-0.39 ± 0.2	1.05 ± 0.2 (σ^*)	-0.5 ± 0.3 ($3p'$)

been made here on a basis of qualitative interpretation. For quantitative understanding of symmetry of *K*-shell excited states, detailed theoretical work is required in connection with experimental studies.

IV. SUMMARY

The angular distributions for the combined signal of N^+ and O^+ and for that of N^{2+} and O^{2+} from NO have been measured near the N *K* edge and the O *K* edge for the first time. The β parameters at N $1s \rightarrow 2p \pi^*$ and O $1s \rightarrow 2p \pi^*$ are both close to -1 . The β parameter in the

region of N $1s \rightarrow$ Rydberg orbital transitions varies due to the symmetry of excitations. At about 3.5 eV above the N $1s$ ionization and the O $1s$ ionization thresholds, the β parameter shows a broad maximum due to the σ^* shape resonance.

ACKNOWLEDGMENTS

The authors are grateful to Dr. Tomimasu and the members of the accelerator group of the Electrotechnical Laboratory for providing synchrotron radiation. We are indebted to Dr. Hitchcock for stimulating comments.

-
- ¹J. L. Dehmer and D. Dill, *J. Chem. Phys.* **65**, 5327 (1976).
²T. N. Rescigno and P. W. Langhoff, *Chem. Phys. Lett.* **51**, 65 (1977).
³F. Sette, J. Stöhr, and A. P. Hitchcock, *J. Chem. Phys.* **81**, 4906 (1984).
⁴R. N. Zäre, *Mol. Photochem.* **4**, 1 (1972).
⁵N. Saito and I. H. Suzuki, *Phys. Rev. Lett.* **61**, 2740 (1988).
⁶A. Yagishita, H. Maezawa, M. Ukai, and E. Shigemasa, *Phys. Rev. Lett.* **62**, 36 (1989).
⁷N. Saito and I. H. Suzuki, *J. Phys. B* **22**, 3973 (1989).
⁸N. Saito and I. H. Suzuki, *J. Phys. B* **22**, L517 (1989).
⁹W. Eberhardt, E. W. Plummer, I.-W. Lyo, R. Carr, and W. F. Ford, *Phys. Rev. Lett.* **58**, 207 (1987).
¹⁰N. H. F. Beebe, E. W. Thulstrup, and A. Andersen, *J. Chem. Phys.* **64**, 2080 (1976).
¹¹V. N. Akimov, A. S. Vinogradov, and T. M. Zimkina, *Opt. Spektrosk.* **53**, 109 (1982) [*Opt. Spectrosc. (USSR)* **53**, 63 (1982)].
¹²Y. Morioka, M. Nakamura, E. Ishiguro, and M. Sasanuma, *J. Chem. Phys.* **61**, 1426 (1974).
¹³G. R. Wight and C. E. Brion, *J. Electron Spectrosc. Relat. Phenom.* **4**, 313 (1974).
¹⁴T. Tomimasu, T. Noguchi, S. Sugiyama, T. Yamazaki, T. Mikado, and M. Chiwaki, *IEEE Trans. Nucl. Sci.* **30**, 3133 (1983).
¹⁵N. Saito, I. H. Suzuki, H. Onuki, and M. Nishi, *Rev. Sci. Instrum.* **60**, 2190 (1989).
¹⁶N. Saito and I. H. Suzuki, *Int. J. Mass Spectrom. Ion Processes* **82**, 61 (1988).
¹⁷W. E. Moddeman, T. A. Carlson, M. O. Krause, B. P. Pullen, W. E. Bull, and G. K. Schweitzer, *J. Chem. Phys.* **55**, 2317 (1971).
¹⁸I. H. Suzuki and N. Saito, *J. Chem. Phys.* **91**, 5324 (1989).
¹⁹N. Saito and I. H. Suzuki, *J. Chem. Phys.* **91**, 5329 (1989).
²⁰D. M. Curtis and J. H. D. Eland, *Int. J. Mass Spectrom. Ion Processes* **63**, 241 (1985).